

Patterns of large multilamellar vesicular clusters

T. Lahiri, A. K. Dasgupta and A. Chakrabarti^{†*}

Department of Biochemistry and Biophysics, University of Kalyani, Nadia 741 235, India

[†]Biophysics Division, Saha Institute of Nuclear Physics, 37 Belgachia Road, Calcutta 700 037, India

Digitized images of dimyristoyl phosphatidylcholine (DMPC) vesicular clusters, obtained from ordinary bright field microscopy were studied. The clusters followed certain scaling behaviour and could be characterized by the mass fractal dimension D and the porosity value P . Structural perturbations caused by the presence of the cytoskeletal protein, spectrin and hydrodynamic perturbations caused by dilution resulted in change in the above mentioned parameters. The results suggest that the collective behaviour of phospholipid vesicles can serve as an important tool to detect minor alterations in the microenvironment.

CLUSTER formation is a phenomenon which has drawn substantial interest from a wide variety of disciplines¹⁻⁷. Clusters can either be spanned (finite) or unspanned depending on whether the aggregate is bound or unbound within a given spatial domain. Contrary to the notion that the clustered assemblies are non-classifiable due to their random formation, it is now believed that minor changes in local interactions or initial conditions may lead to systematic changes in the geometric properties of clusters. Phospholipid vesicles, liposomes, have been widely used as a model system for the study of problems associated with the bilayer membranes, but clusters of spontaneously formed phospholipid vesicles are yet to be classified. We have studied such vesicle clusters under a brightfield microscope by image processing and subsequent analysis of such images to obtain the characteristic parameters for the clusters. In this report we examine the effect of dilution and structural perturbations caused by a cytoskeletal protein, spectrin, known to provide morphological integrity to the erythrocyte membranes.

Dried films of dimyristoyl phosphatidylcholine (DMPC) (Sigma) were hydrated in a buffer containing 5 mM phosphate, 20 mM KCl, 1 mM EDTA, 0.2 mM DTT, pH 8.0, with and without spectrin (200 µg/ml) to form multilamellar DMPC (4 mM) vesicles. White ghosts from goat blood were prepared by hypotonic lysis in 5 mM phosphate, 1 mM EDTA containing 20 µg/ml of PMSF at pH 8.0, following the procedure of Dodge and co-workers⁸. Spectrin was removed from the ghosts in a buffer containing 0.2 mM sodium phosphate, 0.1 mM EDTA, 0.2 mM DTT, 20 µg/ml of PMSF, pH 8.0

at 37°C. Spectrin dimers were purified after 30% ammonium sulphate precipitation by following published protocols⁹.

The DMPC vesicles, after an hour of incubation at room temperature, were spread on a glass slide, and were visualized through the bright field of an ordinary microscope (Model Diastar, Reichert Scientific Instrument, USA). At least four different fields of view were visually scanned to test the gross uniformity of the resultant clusters. The computer-grabbed images were imported into Windows environment (Microsoft Corporation, USA) using MATLAB under Windows (MathWorks Inc., USA). Figures 1 *a* and *b* show the digitized grey images of the DMPC vesicles in absence and presence of spectrin.

Image processing was performed by Image Processing Toolbox procured from MathWorks. In most cases, however, routines specific for the problem, were developed. For processing the indexed images, the first step was thresholding. The optimal choice for threshold grey value was made following the reported method with minor modifications¹⁰⁻¹², where the histogram of grey value of each pixel was taken with 50 number of bins. Then, the overall extraction was carried out with the grey value corresponding to the bin which is 4th in position regarding frequency.

Once the thresholded image is obtained, one may obtain two classes of information. Firstly, one might ignore the porosity space and observe the cluster contour. Secondly, one might be interested in following up how the image pattern changes by rescaling (i.e. by sampling the image points in frame, with an altered grid distribution). Thus the original grey level image in Figure 1 *a* is subjected to thresholding in Figure 2 *a*, which contains the binary information about the porous region as well as the cluster contour. Figure 2 *b* represents the clusters without any indication to the porous region. Rescaling has been illustrated in Figure 2 *c*, which shows how scaling alters the thresholded image (Figure 2 *a*).

To measure the cluster area including pores (A) from the binary image (i.e. to generate Figure 2 *b* from Figure 2 *a*, the image was first fixed in a rectangular frame). To include the porous region in the calculation of area, the following overlay method was followed. Eight separate images were generated by unit pixel translation parallel to positive and negative directions of abscissa keeping the ordinate fixed, parallel to positive and negative directions of ordinate keeping the abscissa fixed and parallel to the four diagonal of the image frame respectively. The translated image points were layered on top of one another and the union of all such points was called the image O' (data for Figure 2 *b*). To obtain rescaled image (Figure 2 *c*), the image co-ordinates were subjected to suitable scaling transformations.

To get the mass fractal dimensions of the clusters we

*For correspondence

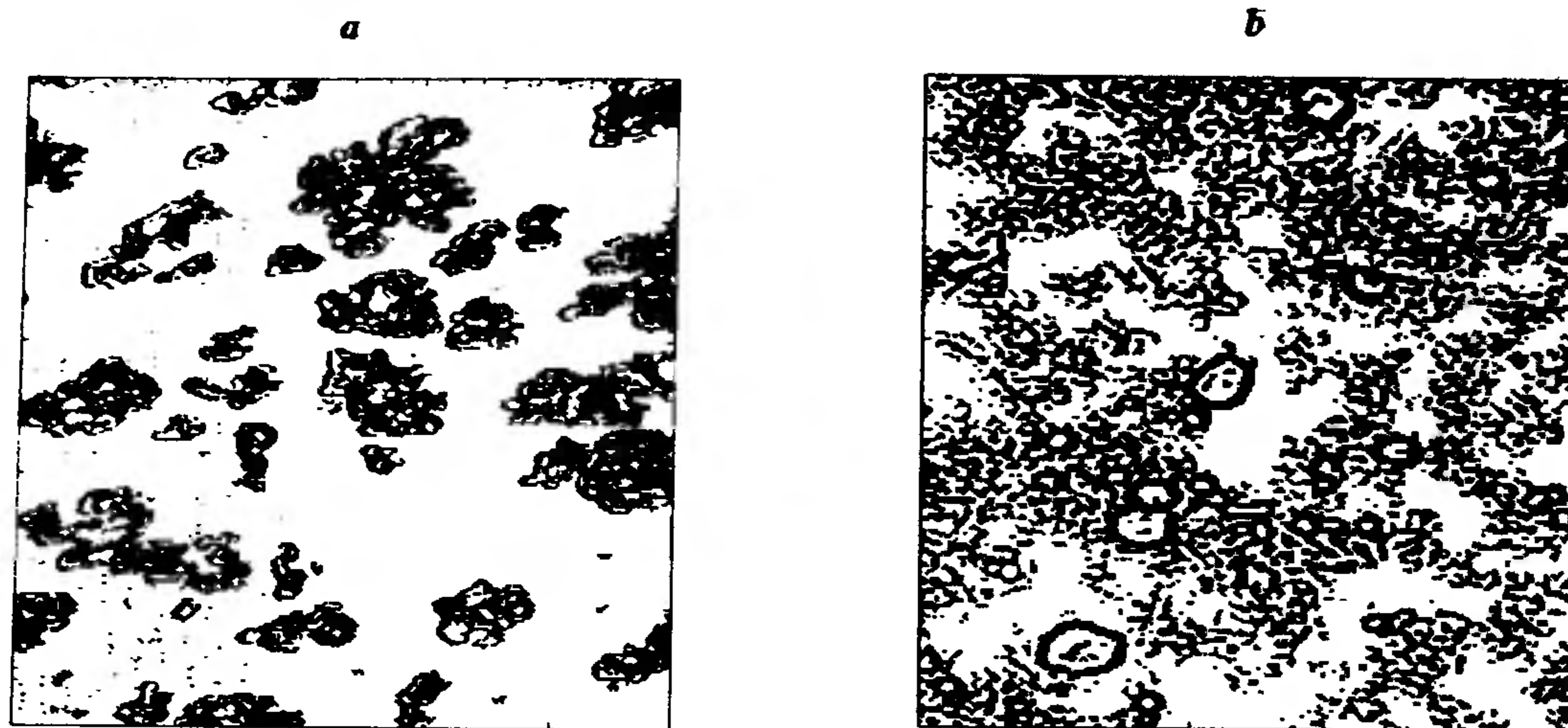


Figure 1 *a, b*. Clusters of DMPC vesicles in (*a*) absence and (*b*) presence of spectrin.

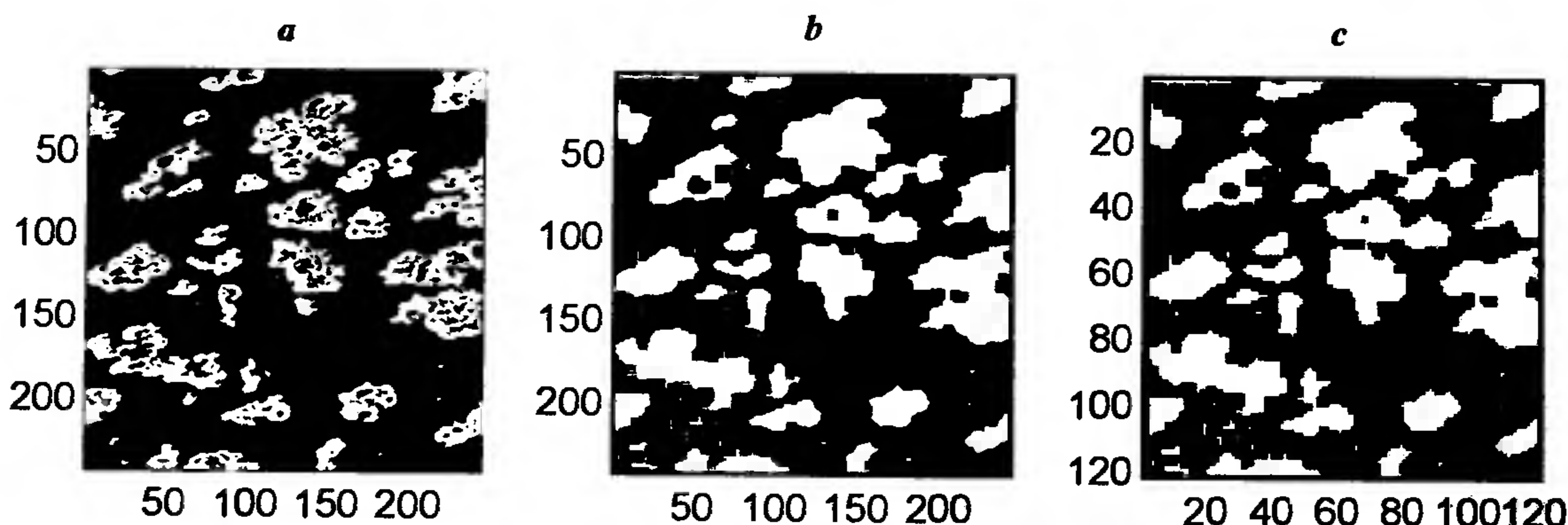


Figure 2 *a-c*. Different stages of processed images (*a*) binary image conversion after thresholding, (*b*) image showing the area within the total cluster contour and (*c*) rescaled image with length scale elongated two-fold (10 pixels = 13.9 μm).

resized all the input thresholded binary images. For this, the input image was scanned blockwise (size of each block was assumed as $a \times a$) each time checking the total grey value, G of each block with the following rule:

if,

$$G(i, j) > 0 \text{ then } R(i, j) = 1; \text{ else } R(i, j) = 0,$$

endif,

where the scale length was represented by a , the size of the input image matrix was m and the size of the output image, R (Figure 2 *c*) was, $L = m/a$. The cluster mass, M (number of white pixels, or occupied sites) of the resized images was measured at different lattice sizes, L ($L = 4, 6, 8, 10, 12, 16, 20, 24, 28$ and 32

pixels). The exponent, D , could be obtained from the equation given by¹³:

$$M = L^D, \tag{1}$$

where the slope of the linear fit of $\ln(M)$ plotted against $\ln(L)$ gives the measure of D , shown in Figure 3.

To evaluate the porosity of the clusters from their two-dimensional view, the expression of the porosity in the three-dimensional space^{14,15} might be modified as

$$P = 1 - A_1/A, \tag{2}$$

where A is the overall cluster area and A_1 is the area excluding the pore space.

DMPC films upon hydration with the aqueous buffer

formed large multilamellar vesicles, which upon incubation at 25°C formed stable clusters. When spread on the microscopic slides, spanned clusters were observed without any relative movement between the cluster components. The clustered patterns remained visually similar even when the microscopic slide was physically shifted in the x - y plane. We have obtained a good linear fit in the plots of $\ln(L)$ and $\ln(M)$ (Figure 3), both in absence and presence of spectrin. In the initial stock solution the D value was notably higher in presence of spectrin than that in the absence. After two-fold dilution, a decrease in D was observed in presence of spectrin (200 $\mu\text{g/ml}$), while the D remained unchanged in its absence (Table 1). However, a gradual increase in D , at 2-fold dilution, was evident with the increasing concentrations of spectrin (Figure 3 *b*). Data for evaluation of porosity P , were collected from the threshold-image using eq. (2). For stock solutions we found the mean value of P for clusters of DMPC vesicles to be much lower in the absence of spectrin than that in the presence of spectrin. After two-fold dilution the mean value of P significantly increased for the clusters without spectrin. But on contrary, after 2-fold dilution P remained almost unchanged in the presence of spectrin.

As we see from Table 1, the mean mass fractal dimension, D for the stock DMPC vesicular suspension was significantly lowered (≈ 1.662) in the absence of spectrin than in presence of spectrin (≈ 2.0). The magnitude of D implied that for the DMPC vesicular clusters including the cytoskeletal protein, spectrin, the cluster formation is above the limit of percolation threshold. The cluster formation is below the limit of percolation

threshold when spectrin was not included in the phospholipid vesicles¹³. A gradual increase of D was observed with the increase in spectrin concentration (100–400 $\mu\text{g/ml}$), implying retention of stability in presence of spectrin (Figure 3). Furthermore, for stable clusters one would expect conservation of the geometric properties even in presence of hydrodynamic perturbation. In presence of spectrin the porosity coefficient P , remains relatively insensitive to dilution. This provides an additional support to the earlier conjecture.

Spectrin is the cytoskeletal protein known to provide morphological integrity to the erythrocyte membranes¹⁶. Earlier studies have shown altered vesicular geometry in presence of structural proteins^{17,18}. Most of such studies were confined to the analysis of individual liposomes. Spectrin is known for its membrane adhesive properties and results presented here do support that spectrin confers more stability to the overall cluster characteristics formed by multilamellar DMPC vesicles. The simple methodology presented here might be useful in characterizing clusters from their geometry, despite ambiguity and variety in the microscopic appearances

Table 1. Mean and standard deviation of fractal index and porosity in absence (-) and presence (+) of spectrin

Fractal index (D)		Porosity (P)	
- Spectrin	+ Spectrin	- Spectrin	+ Spectrin
1.66 ± 0.02 (1.69 ± 0.01)	2.02 ± 0.03 (1.75 ± 0.01)	0.16 ± 0.02 (0.45 ± 0.04)	0.44 ± 0.01 (0.39 ± 0.005)

Values in parenthesis correspond to the same after two-fold dilution.

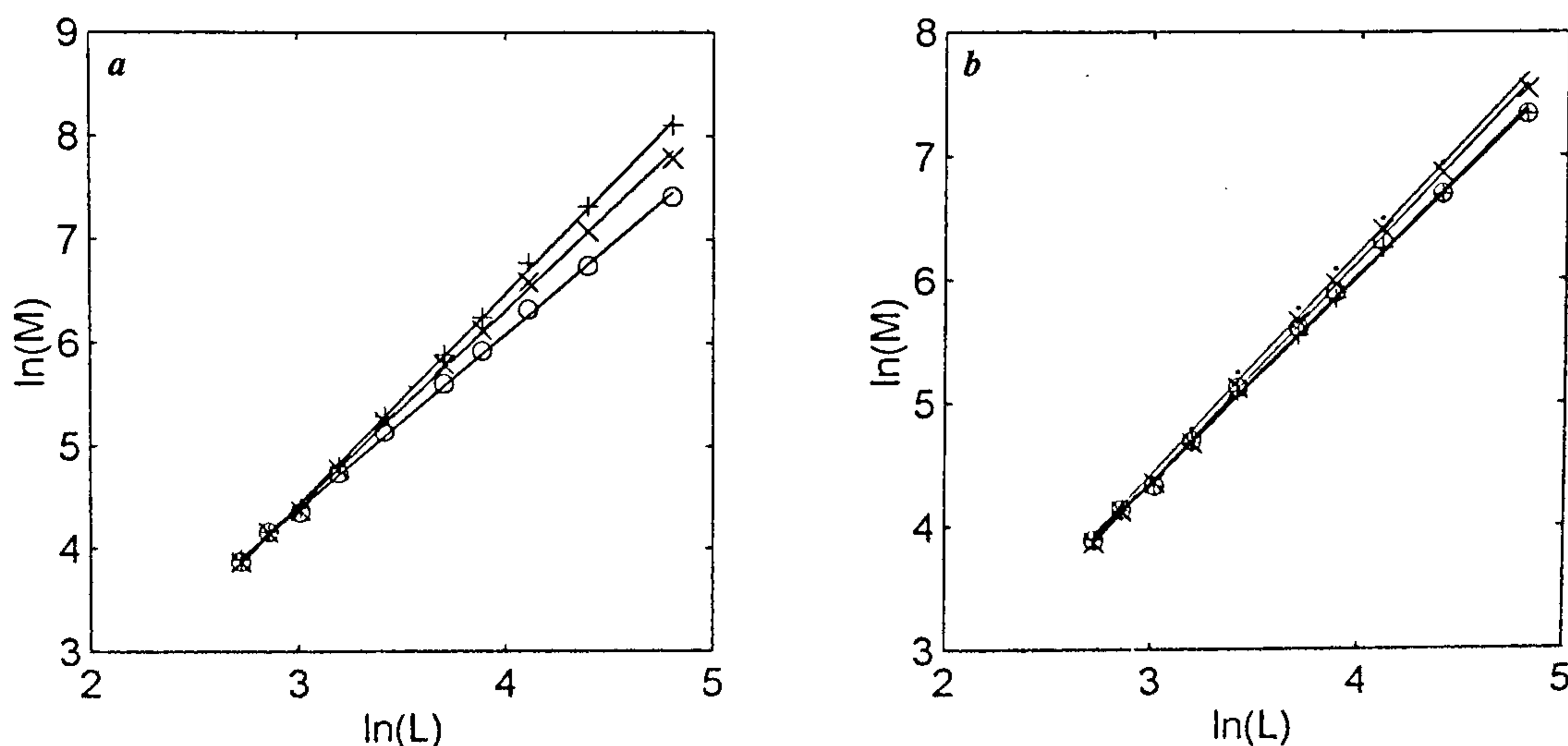


Figure 3 *a, b*. Plot of $\ln(M)$ against $\ln(L)$. Stock vesicular suspension and two-fold dilution of the same are represented by *a* and *b* respectively. The symbols 'O', '+', 'x' and '*' represent spectrin concentration of 0, 100, 200 and 400 μg per ml respectively.

of their individual vesicular forms. The property of clusters responding to the minute perturbing changes in the individual constituting members, might be, in our view, an important tool in the study of cellular or vesicular assembly processes.

1. Jullien, R. and Botet, R., *Aggregation and Fractal Aggregates*, World Scientific, Singapore, 1987.
2. Meakin, P., *Phys. Rev.*, 1987, **A35**, 2234–2245.
3. Meakin, P., in *Fractal Aggregates and their Fractal Measures. Phase Transitions and Critical Phenomena* (eds Domb, C. and Lebowitz, J. L.), Academic Press, New York, 1987.
4. Feder, J., Jøssang, T. and Rosenqvist, E., *Phys. Rev. Lett.*, 1984, **53**, 1403–1406.
5. Jøssang, T., Feder, J. and Rosenqvist, E., *J. Chem. Phys.*, 1984, **120**, 1–30.
6. Feder, J. and Jøssang, T., in *Scaling Phenomena in Disordered Systems* (eds Pynn, R. and Skjeltorp, A.), Plenum Press, New York, 1985, pp. 99–131.
7. Weitz, D. A. and Oliveria, M., *Phys. Rev. Lett.*, 1984, **52**, 1433–1436.
8. Dodge, J. T., Mitchell, C. and Hanahan, D. J., *Arch. Biochem. Biophys.*, 1963, **100**, 119–130.

9. Gratzel, W. B., *Methods Enzymol.*, 1985, **85**, 475–480.
10. Gonzalez, R. C. and Wintz, P. A., *Digital Image Processing*, Addison-Wesley, Massachusetts, USA, 1979.
11. Pal, S. K. and Bhattacharyya, A., *Pattern Recog. Lett.*, 1990, **11**, 443–452.
12. Thompson, C. M. and Shure, L., *Image Processing Toolbox User's Guide*, The Math Works Inc., Natick, MA, USA, 1993.
13. Feder, J., *Fractals*, Plenum, New York, 1988, Chapter 7 & 12.
14. Witten, T. A. and Cates, M. E., *Science*, 1986, **232**, 1607–1610.
15. Logan, E. and Wilkinson, D. B., *Biotechnol. Bioeng.*, 1991, **38**, 389–396.
16. Bennet, V., *Annu. Rev. Biochem.*, 1985, **54**, 273–310.
17. Miyata, H. and Hotani, H., *Proc. Natl. Acad. Sci. USA.*, 1992, **89**, 11547–11551.
18. Sackmann, E., *FEBS Lett.*, 1994, **346**, 3–16.

ACKNOWLEDGEMENTS. T. Lahiri is a recipient of Senior Research Fellowship from Indian Council of Medical Research. We thank Dr Indrani Bose, Dr Bikash Chakrabarti and Mr N. S. Kar for their help and co-operation. This work was partially supported by a grant from Council of Scientific and Industrial Research, New Delhi, to A. Dasgupta.

Received 20 July 1996; revised accepted 25 October 1996

The plant Banjauri (*Vicoa indica*) exhibits antifertility activity in adult female bonnet monkeys (*Macaca radiata*)

A. J. Rao*, N. Ravindranath[†] and N. R. Moudgal

Primate Research Laboratory, Center for Reproductive Biology and Molecular Endocrinology, Indian Institute of Science, Bangalore 560 012, India

[†]Department of Anatomy and Cell Biology, George Town University Medical Center, 3900 Reservoir Road, NW, Washington DC 2007, USA

The antifertility activity of the plant *Vicoa indica* was tested in proven fertile bonnet monkeys. The dry powder of the whole plant was fed to the cycling monkeys on day 1 to 14 of menstrual cycle or day 9 to 14 of cycle or on day 2 to 5 after delivery and the fertility was evaluated in the following cycle in cycle fed monkey or after weaning the young one in the post-partum fed monkeys. Results indicated that while feeding in the post-partum monkeys did not confer any protection against pregnancy feeding during day 1 to 14 of cycle, protected from pregnancy. The monkeys did not become pregnant even after exposure to the proven fertile male monkeys for 13 ovulatory cycles while all the vehicle fed monkeys became pregnant within 3 cycles.

BANJAURI is the colloquial name for the plant *Vicoa indica* which belongs to the family Compositae. It is a

*For correspondence

small plant of about 1–2 feet height with slender stem, long leaves and small yellow flowers. The plant grows wild in the months of July/August and fully mature plants with flowers are seen during September/October. It is reported¹ that the Adivasi tribes in Bihar use Banjauri as a contraceptive. According to the practice followed by Adivasis, the freshly collected plant is sun-dried and the whole plant equivalent is powdered along with seven pepper seeds and consumed each day as a suspension in water by woman on the second to fifth day after delivery of the child or from day 1 to 14 of three consecutive menstrual cycles. Such treatment reportedly induces permanent sterility. In view of the nonavailability of scientifically documented clinical study on the use of Banjauri, we have attempted to verify the activity profile of this plant product by determining the effect of feeding dried Banjauri powder both during post-partum period and early phase of the menstrual cycle on fertility of proven fertile adult female bonnet monkeys.

The procedures adopted for care and maintenance of bonnet monkeys have been reported in detail earlier². The serum levels of estradiol-17 β , progesterone and chorionic gonadotropin were determined according to methods described earlier³.

Dried plant material was powdered and passed through a metal sieve (500 μ mesh) to remove coarse fibrous material. The finely powdered material was mixed with groundnut seeds and brown sugar in a ratio of (1:4:8) and thoroughly ground in a mortar and the resulting paste was fed to the monkeys. Care was taken